

# Discovering a Light Higgs Boson with Light

Greg Landsberg<sup>1</sup> and Konstantin T. Matchev<sup>2</sup>

<sup>1</sup>*Physics Department, Brown University, 182 Hope St, Providence, RI 02912*

<sup>2</sup>*Theoretical Physics Department, Fermi National Accelerator Laboratory, Batavia, IL 60510*

**Abstract.** We evaluate the prospects for detecting a non-standard light Higgs boson with a significant branching ratio to two photons, in the Run II of the Fermilab Tevatron. We derive the reach for several channels:  $2\gamma$  inclusive,  $2\gamma + 1$  jet, and  $2\gamma + 2$  jets. We present the expected Run II limits on the branching ratio of  $h \rightarrow \gamma\gamma$  as a function of the Higgs mass, for the case of “bosonic”, as well as “topcolor” Higgs bosons.

## MOTIVATION

The Standard Model (SM) is very economical in the sense that the Higgs doublet responsible for electroweak symmetry breaking can also be used to generate fermion masses. The Higgs boson couplings to the gauge bosons, quarks, and leptons are therefore predicted in the Standard Model, where one expects the Higgs boson to decay mostly to b-jets and tau pairs (for low Higgs masses,  $M_h \lesssim 140$  GeV), or to  $WW$  or  $ZZ$  pairs, (for higher Higgs masses,  $M_h \gtrsim 140$  GeV). Since the Higgs boson is neutral and does not couple to photons at tree level, the branching ratio  $B(h \rightarrow \gamma\gamma)$  is predicted to be very small in the SM, on the order of  $10^{-3} - 10^{-4}$ .

In a more general framework, however, where different sectors of the theory are responsible for the physics of flavor and electroweak symmetry breaking, one may expect deviations from the SM predictions, which may lead to drastic changes in the Higgs boson discovery signatures. One such example is the so called “fermiophobic” (also known as “bosophilic” or “bosonic”) Higgs, which has suppressed couplings to all fermions. It may arise in a variety of models, see e.g. [1]. A variation on this theme is the Higgs in certain topcolor models, which may couple to heavy quarks only [2]. Some even more exotic possibilities have been suggested in the context of theories with large extra dimensions [3]. Finally, in the minimal supersymmetric standard model (MSSM), the width into  $b\bar{b}$  pairs can be suppressed due to 1-loop SUSY corrections, thus enhancing the branching ratios of a light Higgs into more exotic signatures [4,5]. In all these cases, the Higgs boson decays to photon pairs are mediated through a  $W$  or heavy quark loop and dominate for  $M_h \lesssim 100$  GeV [6]. In the range  $100 \lesssim M_h \lesssim 160$ , they compete with the  $WW^*$  mode, while for  $M_h \gtrsim 160$  GeV,  $h \rightarrow WW$  completely takes over. Current bounds from LEP [7] are limited by the kinematic reach of the machine. The existing Run I analyses at the Tevatron have utilized the diphoton plus 2 jets [8–10] and inclusive diphoton [10] channels and were limited by statistics. Since they only looked for a “bosonic” Higgs [1], they did not consider the Higgs production mechanism through gluon fusion, which can be a major additional source of signal in certain models [2]. Since  $h \rightarrow \gamma\gamma$  is a very clean signature, it will allow the Tevatron to extend significantly those limits in its next run.

In this study we shall evaluate the Higgs discovery potential of the upcoming Tevatron runs for several diphoton channels. We shall concentrate on the following two questions. First, what is the absolute reach in Higgs mass as a function of the  $h \rightarrow \gamma\gamma$  branching ratio? Second, which signature (inclusive diphotons, diphotons plus one jet, or diphotons plus two jets) provides the best reach. We believe that neither of those two questions has been adequately addressed in the literature previously.

## TEVATRON REACH FOR A BOSONIC HIGGS

Here we consider the case of a “bosonic” Higgs, i.e. models where the Higgs couplings to all fermions are suppressed. Then, the main Higgs production modes at the Tevatron are associated  $Wh/Zh$  production, as well as  $WW/ZZ$

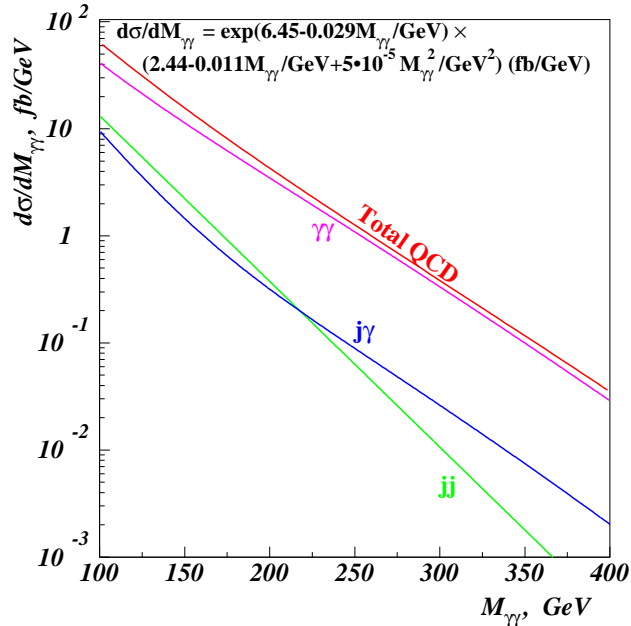


**FIGURE 1.** The total background in the inclusive diphoton channel, as well as the individual contributions from  $\gamma\gamma$ ,  $j\gamma$  and  $jj$  production.

fusion. All of these processes have comparable rates [11], so it makes sense to consider an inclusive signature first [10].

### Inclusive channel: analysis cuts

We use the following cuts for our inclusive study: two photons with  $p_T(\gamma) > 20$  GeV and rapidity  $|\eta(\gamma)| < 2$ , motivated by the acceptance of the CDF or DØ detectors in Run II. Triggering on such a signature is trivial; both collaborations will have diphoton triggers that are nearly fully efficient with such offline cuts.

We assume 80% diphoton identification efficiency, which we apply to both the signal and background estimates on top of the kinematic and geometrical acceptance. Again, this efficiency is motivated by the CDF/DØ EM ID efficiency in Run I and is not likely to change in Run II.

### Inclusive channel: background

The main backgrounds to the inclusive diphoton channel come from the QCD production of dijets, direct photons, and diphotons. In the former two cases a jet mimics a photon by fragmenting into a leading  $\pi^0/\eta$  meson that further decays into a pair of photons, not resolved in the calorimeter.

We used the PYTHIA [12] event generator and the experimentally measured probability of a jet to fake a photon [8] to calculate all three components of the QCD background. The faking probability depends significantly on the particular photon ID cuts, especially on the photon isolation requirement (see, e.g. [8,13,14]). For this study we used an  $E_T$ -dependent jet-faking-photon probability of

$$P(\text{jet} \rightarrow \gamma) = \exp\left(-0.01 \frac{E_T}{(1 \text{ GeV})} - 7.5\right),$$

which is obtained by taking the  $\eta$ -averaged faking probabilities used in the DØ Run I searches [8]. The fractional error on  $P(\text{jet} \rightarrow \gamma)$  is about 25% and is dominated by the uncertainty on the direct photon fraction in the jet +  $\gamma$  sample used for its determination. (For high photon  $E_T$ , however, the error is dominated by the available statistics.)

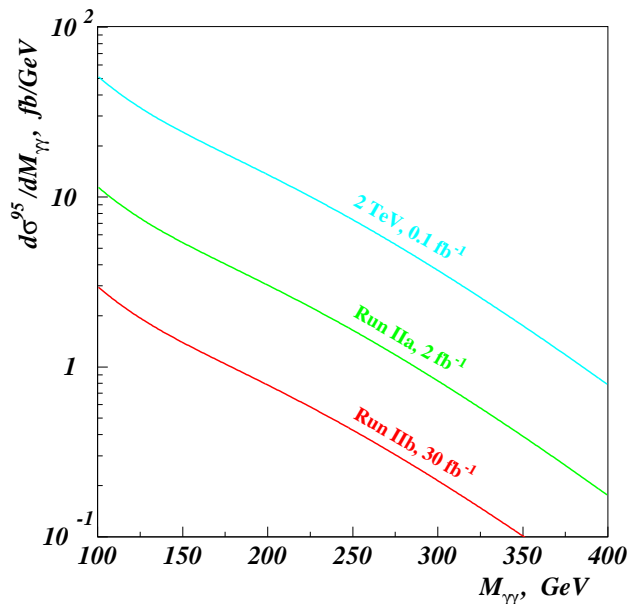


**FIGURE 2.** The 95% CL upper limit on  $\varepsilon \times \sigma(\gamma\gamma + X)$  as a function of  $M_{\gamma\gamma}$ , for several benchmark total integrated luminosities in Run II.

This probability is expected to remain approximately the same in Run II for both the CDF and DØ detectors. We used 80% ID efficiency for the pair of photons, and required the photons to be isolated from possible extra jets in the event. We accounted for NLO corrections via a constant  $k$ -factor of 1.34.

Adding all background contributions, for the total background in the inclusive diphoton channel we obtain the following parametrization:

$$\frac{d\sigma}{dM_{\gamma\gamma}} = \left[ p_3 + p_4 \left( \frac{M_{\gamma\gamma}}{1 \text{ GeV}} \right) + p_5 \left( \frac{M_{\gamma\gamma}}{1 \text{ GeV}} \right)^2 \right] \exp \left\{ p_1 + p_2 \left( \frac{M_{\gamma\gamma}}{1 \text{ GeV}} \right) \right\},$$

where  $p_1 = 6.45$ ,  $p_2 = -0.029$ ,  $p_3 = 2.44$ ,  $p_4 = -0.011$  and  $p_5 = 0.00005$ . In the region  $M_{\gamma\gamma} > 100$  GeV it is dominated by direct diphoton production and hence is irreducible. The expected statistical plus systematic error on this background determination is at the level of 25%, based on the jet-faking photon probability uncertainty. For larger invariant masses, however, the accuracy is dominated by the uncertainties in the direct diphoton production cross section, which will be difficult to measure independently in Run II, so one will still have to rely on the NLO predictions. On the other hand, for narrow resonance searches one could do self-calibration of the background by calculating the expected background under the signal peak via interpolation of the measured diphoton mass spectrum between the regions just below and just above the assumed resonance mass. Therefore, in our case the background error will be purely dominated by the background statistics. A combination of the interpolation technique and the shape information from the theoretical NLO calculations of the direct diphoton cross section is expected to result in significantly smaller background error in Run II.

The total background, as well as the individual contributions from  $\gamma\gamma$ ,  $\gamma j$  and  $jj$  production, are shown in Fig. 1. Additional SM background sources to the inclusive diphoton channel include Drell-Yan production with both electrons misidentified as photons,  $W\gamma\gamma$  production, etc. and are all negligible compared to the QCD background. The absolute normalization of the background obtained by the above method agrees well with the actual background measured by CDF and DØ in the diphoton mode [10,14].

In Fig. 2 we show the 95% CL upper limit on the differential cross section after cuts  $d(\varepsilon \times \sigma(\gamma\gamma + X))/dM_{\gamma\gamma}$  as a function of the diphoton invariant mass  $M_{\gamma\gamma}$ , given the above background prediction (here  $\varepsilon$  is the product of the acceptance and all efficiencies). This limit represents  $1.96\sigma$  sensitivity to a narrow signal when doing a counting experiment in 1 GeV diphoton mass bins. This plot can be used to obtain the sensitivity to any resonance decaying into two photons as follows. One first fixes the width of the mass window around the signal peak which is used in

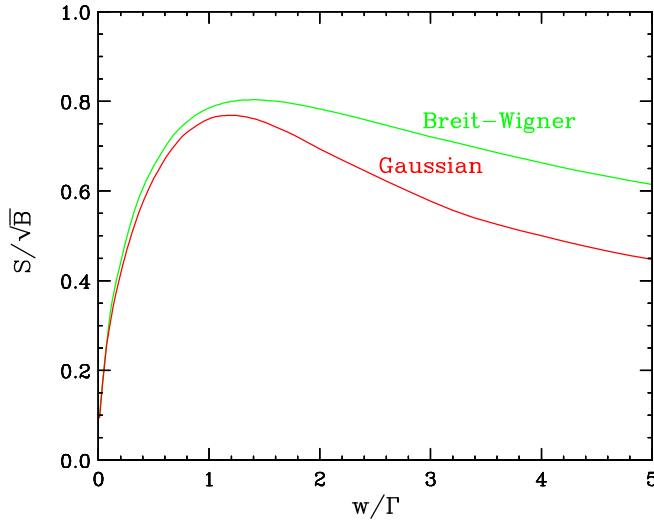


**FIGURE 3.** Significance  $S/\sqrt{B}$  (in arbitrary units), as a function of the mass window width  $w$  (in units of  $\Gamma$ ), for a Breit-Wigner or Gaussian resonance.

the analysis. Then one takes the average value of the 95% C.L. limit in  $d\sigma/dM_{\gamma\gamma}$  across the mass window from Fig. 2 and multiplies it by  $\sqrt{w/\text{GeV}}$ , where  $w$  is the width of the mass window<sup>1</sup>, to obtain the corresponding 95% CL upper limit on the signal cross-section after cuts. Similar scaling could be used if one is interested in the  $3\sigma$  or  $5\sigma$  reach.

### What is the optimum mass window cut?

When searching for narrow resonances in the presence of large backgrounds ( $B$ ), the best sensitivity toward signal ( $S$ ) is achieved by performing an unbinned maximum likelihood fit to the sum of the expected signal and background shapes. However, simple counting experiments give similar sensitivity if the size of the signal “window” is optimized. For narrow resonances the observed width<sup>2</sup>  $\Gamma$  is dominated by the instrumental effects, and is often Gaussian. The background in a narrow window centered on the assumed position  $M_0$  of the peak in the signal invariant mass distribution could be treated as linear. Therefore, the Gaussian significance of the signal,  $S/\sqrt{B}$ , as a function of the window width,  $w$ , is given by:

$$\frac{S}{\sqrt{B}} \sim \frac{1}{\sqrt{w}} \frac{1}{\sqrt{2\pi}\sigma} \int_{M_0-w/2}^{M_0+w/2} d\sqrt{s} \exp\left(-\frac{(\sqrt{s}-M_0)^2}{2\sigma^2}\right) \sim \frac{1}{\sqrt{w/\Gamma}} \text{erf}\left(\sqrt{\ln 2} \frac{w}{\Gamma}\right), \quad (1)$$

where  $\text{erf}(x)$  is the error function

$$\text{erf}(x) = \frac{2}{\sqrt{\pi}} \int_0^x e^{-t^2} dt.$$

The function (1) is shown in Fig. 3, and has a maximum at  $w \approx 1.2\Gamma$ , which corresponds to  $\pm 1.2(\Gamma/2)$  cut around the resonance maximum.

For resonances significantly wider than the experimental resolution, the shape is given by the Breit-Wigner function, and in this case the significance is:

$$\frac{S}{\sqrt{B}} \sim \frac{1}{\sqrt{w}} \int_{(M_0-w/2)^2}^{(M_0+w/2)^2} \frac{ds}{(s-M_0^2)^2 + M_0^2\Gamma^2} \sim \frac{1}{\sqrt{w/\Gamma}} \arctan\left(\frac{w}{\Gamma}\right). \quad (2)$$

<sup>1)</sup> The square root enters the calculation since the significance is proportional to the background to the  $-1/2$  power.

<sup>2)</sup> Notice that the width is defined so that the cross-section at  $\pm\Gamma/2$  away from the peak is a factor of 2 smaller than the peak value (FWHM). For a Gaussian resonance the width is related to the variance  $\sigma$  by  $\Gamma = 2\sigma\sqrt{\ln 4} \simeq 2.35\sigma$ .

This function, also shown in Fig. 3, peaks at a similar value of  $w$  ( $w \approx 1.4\Gamma$ ). We see that for both Gaussian and Breit-Wigner resonances, the significance does not appreciably change when using a  $w = 1\Gamma - 2\Gamma$  cuts. For our analysis we shall use two representative choices:  $w = 1.2\Gamma$  and  $w = 2\Gamma$  for the mass window, which we shall always center on the actual Higgs mass.

Clearly, one can do even better in principle, by suitably resizing and repositioning the mass window around the bump in the combined  $S + B$  distribution. Because of the steeply falling parton luminosities, the signal mass peak is skewed and its maximum will appear somewhat below the actual physical mass. In our analysis we choose not to take advantage of these slight improvements, thus accounting for unknown systematics.

## Inclusive channel: results

In Tables 1 and 2 we show the inclusive  $\gamma\gamma + X$  background rates in fb for different Higgs masses, for  $w = 1.2\Gamma$  and  $w = 2\Gamma$  mass window cuts, respectively. Here we have added the intrinsic width  $\Gamma_h$  and the experimental resolution

**TABLE 1.** Background rates in fb for  $w = 1.2\Gamma$  mass cut, and significance ( $S/\sqrt{B}$ , for  $1 \text{ fb}^{-1}$  of data, and assuming  $B(h \rightarrow \gamma\gamma) = 100\%$ ) as a function of the Higgs mass  $M_h$ . The signal consists of associated  $Wh/Zh$  production and  $WW/ZZ$  fusion.

$M_h$ (GeV)	$\gamma\gamma + X$ bknd (fb)	Significance $S/\sqrt{B}$								
		$\gamma\gamma + X$	$\gamma\gamma + 1 \text{ jet}$				$\gamma\gamma + 2 \text{ jets}$			
			$p_T > 20$	$p_T > 25$	$p_T > 30$	$p_T > 35$	$p_T > 20$	$p_T > 25$	$p_T > 30$	$p_T > 35$
100.	271.7	16.5	31.3	34.2	36.3	35.4	31.9	36.4	35.1	31.1
120.	166.6	13.0	24.4	26.7	28.5	28.5	24.7	29.5	29.2	26.7
140.	103.0	10.7	20.1	22.4	23.9	23.9	20.6	24.0	23.7	21.0
160.	64.3	8.9	17.0	19.1	20.1	20.4	17.2	20.2	20.8	19.2
180.	40.5	7.3	13.5	15.0	16.2	16.5	13.6	16.3	16.7	16.2
200.	26.1	5.8	10.6	11.9	12.5	12.7	10.4	12.3	12.7	12.0
250.	9.4	3.7	6.7	7.5	7.9	8.2	6.6	7.9	8.7	8.4
300.	4.8	2.2	3.8	4.3	4.7	4.7	3.6	4.2	4.9	4.7
350.	2.3	1.5	2.8	3.1	3.3	3.3	2.4	2.8	3.0	3.4
400.	1.2	1.0	1.8	2.0	2.0	2.1	1.7	1.7	2.1	2.4

$\Gamma_{\text{exp}} = 2\sqrt{\ln 4} \times \sigma_{\text{exp}} \simeq 2.35 \times 0.15\sqrt{2}\sqrt{E(\gamma)} \simeq 0.35\sqrt{M_h}$  in quadrature:  $\Gamma = (\Gamma_h^2 + \Gamma_{\text{exp}}^2)^{1/2}$ . The width  $\Gamma$  varies between 3.5 GeV for  $M_h = 100$  GeV and 29.0 GeV for  $M_h = 400$  GeV. The two tables also show the significance (for  $1 \text{ fb}^{-1}$  of data, and assuming  $B(h \rightarrow \gamma\gamma) = 100\%$ ) in the inclusive diphoton channel when only associated  $Wh/Zh$  production and  $WW/ZZ \rightarrow h$  fusion are included in the signal sample. We see that (as can also be anticipated from Fig. 3) a  $w = 1.2\Gamma$  cut around the Higgs mass typically gives a better statistical significance, especially for lighter (and therefore more narrow) Higgs bosons.

## Exclusive channels: analysis

The next question is whether the sensitivity can be further improved by requiring additional objects in the event. The point is that a significant fraction of the signal events from both associated  $Wh/Zh$  production and  $WW/ZZ$  fusion will have additional hard objects, most often QCD jets. In Fig. 4 we show the “jet” multiplicity in associated  $Wh$  production, where for detector simulation we have used the SHW package [15] with a few modifications as in [16]. Here we treat “jets” in a broader context, including electrons and tau jets as well.

Previous studies [10,9] have required *two* or more additional QCD jets. Here we shall also consider the signature with at least *one* additional “jet”, where a “jet” is an object with  $|\eta| < 2$ . The advantages of not requiring a second “jet” are twofold. First, in this way we can also pick up signal from  $WW/ZZ \rightarrow h$  fusion, whose cross-section does not fall off as steeply with  $M_h$ , and in fact for  $M_h > 200$  GeV is larger than the cross-section for associated

**TABLE 2.** The same as Table 1, but for a  $w = 2\Gamma$  mass window.

$M_h$ (GeV)	$\gamma\gamma + X$ bknd (fb)	Significance $S/\sqrt{B}$								
		$\gamma\gamma + X$	$\gamma\gamma + 1$ jet				$\gamma\gamma + 2$ jets			
			$p_T > 20$	$p_T > 25$	$p_T > 30$	$p_T > 35$	$p_T > 20$	$p_T > 25$	$p_T > 30$	$p_T > 35$
100.	453.4	14.4	27.0	29.8	31.7	30.6	27.7	31.9	30.5	26.4
120.	278.1	11.3	21.3	23.5	25.1	24.9	21.9	25.5	25.1	22.5
140.	171.9	9.3	17.5	19.5	21.0	21.0	17.7	20.7	21.0	18.5
160.	107.3	8.0	15.1	16.7	18.0	18.2	15.4	17.8	18.2	17.3
180.	67.6	6.6	12.2	13.7	14.6	14.9	12.4	14.3	15.2	14.2
200.	43.6	5.4	10.1	11.4	12.1	12.1	9.9	11.9	12.3	11.1
250.	15.7	3.6	6.5	7.3	7.7	7.8	6.4	7.6	8.5	8.0
300.	8.1	2.1	3.8	4.2	4.6	4.5	3.6	4.3	4.5	4.5
350.	3.9	1.6	2.7	3.0	3.4	3.4	2.6	3.1	3.5	3.1
400.	2.1	1.1	1.9	2.2	2.3	2.4	1.6	2.1	2.6	2.4

$Wh/Zh$  production<sup>3</sup>. Events from  $WW/ZZ \rightarrow h$  fusion typically contain two very hard forward jets, one of which may easily pass the jet selection cuts. In Fig. 5 we show the pseudorapidity distribution of the two spectator jets in  $WW/ZZ \rightarrow h$  fusion (red) and associated  $Wh/Zh$  production (blue). Second, by requiring only one additional jet, we win in signal acceptance. In order to compensate for the corresponding background increase, we shall consider several  $p_T$  thresholds for the additional jet, and choose the one giving the largest significance.

For the exclusive channels we need to rescale the background from Fig. 1 as follows. From Monte Carlo we obtain reduction factors of  $4.6 \pm 0.5$ ,  $6.2 \pm 1.0$ ,  $7.6 \pm 1.4$ , and  $8.6 \pm 1.5$  for the  $\gamma\gamma + 1$  jet channel, with  $p_T(j) > 20, 25, 30$  and  $35$  GeV, respectively. For the  $\gamma\gamma + 2$  jets channel the corresponding background reduction is  $21 \pm 5$ ,  $38 \pm 12$ ,  $58 \pm 21$ , and  $74 \pm 26$ , depending on the jet  $p_T$  cuts. These scaling factors agree well with those from the CDF and DØ data from Run I.

Notice that we choose not to impose an invariant dijet mass ( $M_{jj}$ ) cut for the  $\gamma\gamma + 2$  jets channel. We do not expect that it would lead to a gain in significance for several reasons. First, given the relatively high jet  $p_T$  cuts needed for the background suppression, there will be hardly any background events left with dijet invariant masses below the (very wide)  $W/Z$  mass window. Second, the signal events from  $WW/ZZ$  fusion, which typically comprise about 25 – 30% of our signal, will have a dijet invariant mass distribution very similar to that of the background. Finally, not imposing the  $M_{jj}$  cut allows for a higher signal acceptance because of the inevitable combinatorial ambiguity for the events with  $> 2$  jets.

The significances for the two exclusive channels, with the four different jet  $p_T$  cuts, are also shown in Tables 1 and 2. We see that the exclusive  $\gamma\gamma + 2$  jets channel with  $p_T(j) > 30$  GeV typically gives the largest significance, but our new exclusive  $\gamma\gamma + 1$  jet channel is following very close behind.

## Exclusive channels: results

We are now ready to present our results for the Run II Tevatron reach for a bosonic Higgs. In Fig. 6 we show the 95% CL upper limit on the branching ratio  $B(h \rightarrow \gamma\gamma)$ , with 0.1 (cyan), 2.0 (green) and  $30 \text{ fb}^{-1}$  (red), as a function of  $M_h$ . For each mass point, we compare the significance for both the inclusive as well as the exclusive channels with all the different cuts, and for the limit we choose the channel with the set of cuts providing the best reach. It turns out that for the case at hand the winners are:  $\circ$ :  $2\gamma + 2j$ , with  $p_T(j) > 25$  GeV;  $\square$ :  $2\gamma + 2j$ , with  $p_T(j) > 30$  GeV, and  $\diamond$ :  $2\gamma + 1j$ , with  $p_T(j) > 30$  GeV. In the figure we also show the HDECAY [17] prediction for  $B(h \rightarrow \gamma\gamma)$  in case of a “bosonic” Higgs. The reach shown for  $0.1 \text{ fb}^{-1}$  is intended as a comparison to Run I, in fact for the  $0.1 \text{ fb}^{-1}$  curve we scaled down both the signal and background cross-sections to their values at 1.8 TeV center-of-mass energy, keeping the efficiencies the same. In other words, the region marked as Run I’ would have been the hypothetical reach in Run I, if the improved Run II detectors were available at that time. As seen

<sup>3)</sup> In the case of a topcolor Higgs (see the next section) we would also pick up events with initial state gluon radiation, comprising about 30% of the gluon fusion signal, which is the dominant production process for any Higgs mass.

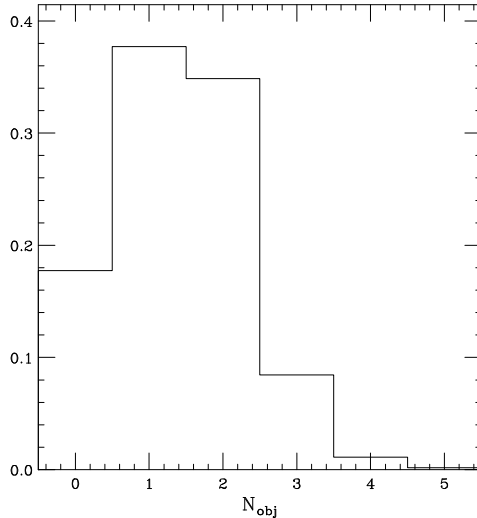


**FIGURE 4.** The number of “jets”, which stands for QCD jets, tau jets and electrons, in associated  $Wh$  production, once we require the two photons from the Higgs to pass the photon ID cuts.

from Fig. 6, the reach for a “bosonic” Higgs [1] (at 95% CL) in Run IIa and Run IIb is  $\sim 115$  GeV and  $\sim 125$  GeV, correspondingly. This is a significant improvement over the ultimate reach from LEP [7] of  $\sim 105$  GeV.

## TEVATRON REACH FOR A TOPCOLOR HIGGS

Here we consider the case of a “topcolor” bosonic Higgs, where the Higgs also couples to the top and other heavy quarks [2]. We therefore include events from gluon fusion into our signal sample. We used the next-to-leading order cross-sections for gluon fusion from the HIGLU program [18].

In Tables 3 and 4 we show the significance (for  $1 \text{ fb}^{-1}$  of data, and again assuming  $B(h \rightarrow \gamma\gamma) = 100\%$ ) in the inclusive and the two exclusive channels, for the topcolor Higgs case. Since gluon fusion, which rarely has additional hard jets, is the dominant production process, the inclusive channel typically provides the best reach. However, the  $2\gamma + 1j$  channel is again very competitive, since the additional hard jet requirement manages to suppress the background at a reasonable signal cost. We see that our new  $2\gamma + 1j$  channel clearly gives a better reach than the  $2\gamma + 2j$  channel [8–10]. For Higgs masses above  $\sim 180$  GeV, it sometimes becomes marginally better even than the inclusive diphoton channel. The specific jet  $p_T$  cut and mass window size  $w$  seem to be less of an issue – from Tables 3 and 4 we see that  $p_T(j) > 25$ ,  $p_T(j) > 30$  GeV and  $p_T(j) > 35$  GeV work almost equally well, and for  $M_h \gtrsim 200$  GeV both values of  $w$  are acceptable.

In Fig. 7 we show the Run II reach for the branching ratio  $B(h \rightarrow \gamma\gamma)$  as a function of the Higgs mass, for the case of a “topcolor” Higgs boson. This time the channels with the best signal-to-noise ratio are:  $\circ$ : inclusive  $2\gamma + X$ , and  $\square$ :  $2\gamma + 1j$ , with  $p_T(j) > 30$  GeV; both with  $w = 1.2\Gamma$ .

## CONCLUSIONS

We have studied the Tevatron reach for Higgs bosons decaying into photon pairs. For purely “bosonic” Higgses, which only couple to gauge bosons, the  $2\gamma + 2j$  channel offers the best reach, but the  $2\gamma + 1j$  channel is almost as good. For topcolor Higgs bosons, which can also be produced via gluon fusion, the inclusive  $2\gamma + X$  channel is the best, but the  $2\gamma + 1j$  channel is again very competitive. We see that in both cases the  $2\gamma + 1j$  channel is a no-lose option!

**Acknowledgments.** We would like to thank S. Mrenna for many useful discussions and B. Dobrescu for comments on the manuscript. This research was supported in part by the U.S. Department of Energy under Grants No. DE-AC02-76CH03000 and DE-FG02-91ER40688. Fermilab is operated under DOE contract DE-AC02-76CH03000.

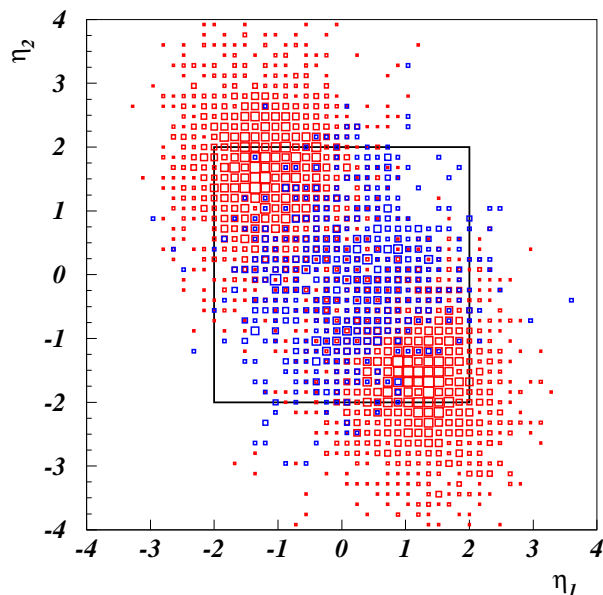


**FIGURE 5.** Pseudorapidity distribution of the two spectator jets in  $WW/ZZ \rightarrow h$  fusion (red) and associated  $Wh/Zh$  production (blue). The boxed region represents the off-line selection cuts.

## REFERENCES

1. H. E. Haber, G. L. Kane and T. Sterling, “The Fermion Mass Scale And Possible Effects Of Higgs Bosons On Experimental Observables,” Nucl. Phys. **B161**, 493 (1979); J. F. Gunion, R. Vega and J. Wudka, “Higgs Triplets In The Standard Model,” Phys. Rev. **D42**, 1673 (1990); J. L. Basdevant, E. L. Berger, D. Dicus, C. Kao and S. Willenbrock, “Final state interaction of longitudinal vector bosons,” Phys. Lett. **B313**, 402 (1993), hep-ph/9211225; V. Barger, N. G. Deshpande, J. L. Hewett and T. G. Rizzo, “A separate Higgs,” preprint OITS-499, hep-ph/9211234; P. Bamert and Z. Kunszt, “Gauge boson masses dominantly generated by Higgs triplet contributions?,” Phys. Lett. **B306**, 335 (1993), hep-ph/9303239. A. G. Akeroyd, “Fermiophobic Higgs bosons at the Tevatron,” Phys. Lett. **B368**, 89 (1996), hep-ph/9511347; M. C. Gonzalez-Garcia, S. M. Lietti and S. F. Novaes, “Search for non-standard Higgs boson in diphoton events at  $p\bar{p}$  collisions,” Phys. Rev. **D57**, 7045 (1998), hep-ph/9711446; A. Barroso, L. Brucher and R. Santos, “Is there a light fermiophobic Higgs?,” Phys. Rev. **D60**, 035005 (1999), hep-ph/9901293; L. Brucher and R. Santos, “Experimental signatures of fermiophobic Higgs bosons,” hep-ph/9907434.
2. B. Dobrescu, “Minimal composite Higgs model with light bosons,” preprint FERMILAB-PUB-99/234-T, hep-ph/9908391; B. Dobrescu, G. Landsberg and K. Matchev, preprint FERMILAB-PUB-99/324-T.
3. L. Hall and C. Kolda, “Electroweak symmetry breaking and large extra dimensions,” Phys. Lett. **B459**, 213 (1999), hep-ph/9904236; H. Cheng, B. A. Dobrescu and C. T. Hill, “Electroweak symmetry breaking and extra dimensions,” preprint FERMILAB-PUB-99/358-T, hep-ph/9912343.
4. M. Carena, S. Mrenna and C. E. Wagner, “MSSM Higgs boson phenomenology at the Tevatron collider,” Phys. Rev. **D60**, 075010 (1999), hep-ph/9808312.
5. S. Mrenna, talk given at PASCOS’99, Lake Tahoe, CA, December 10-16, 1999; S. Mrenna and J. Wells, preprint UCD-2000-02, to appear.
6. A. Djouadi, M. Spira and P. M. Zerwas, “Two photon decay widths of Higgs particles,” Phys. Lett. **B311**, 255 (1993), hep-ph/9305335; A. Stange, W. Marciano and S. Willenbrock, “Higgs bosons at the Fermilab Tevatron,” Phys. Rev. **D49**, 1354 (1994), hep-ph/9309294; M. A. Diaz and T. J. Weiler, “Decays of a fermiophobic Higgs,” preprint VAND-TH-94-1, hep-ph/9401259; K. Melnikov, M. Spira and O. Yakovlev, “Threshold effects in two photon decays of Higgs particles,” Z. Phys. **C64**, 401 (1994), hep-ph/9405301; S. Moretti and W. J. Stirling, “Contributions of below threshold decays to MSSM Higgs branching ratios,” Phys. Lett. **B347**, 291 (1995), hep-ph/9412209; Y. Liao and X. Li, “ $O(\alpha^2 G_F m_t^2)$  contributions to  $H \rightarrow \gamma\gamma$ ,” Phys. Lett. **B396**, 225 (1997), hep-ph/9605310; M. Steinhauser, “Corrections of  $O(\alpha_s^2)$  to the decay of an intermediate-mass Higgs boson into two photons,” preprint MPI-PHT-96-130, hep-ph/9612395; A. Djouadi, “Decays of the Higgs bosons,” preprint PM-97-51, hep-ph/9712334.

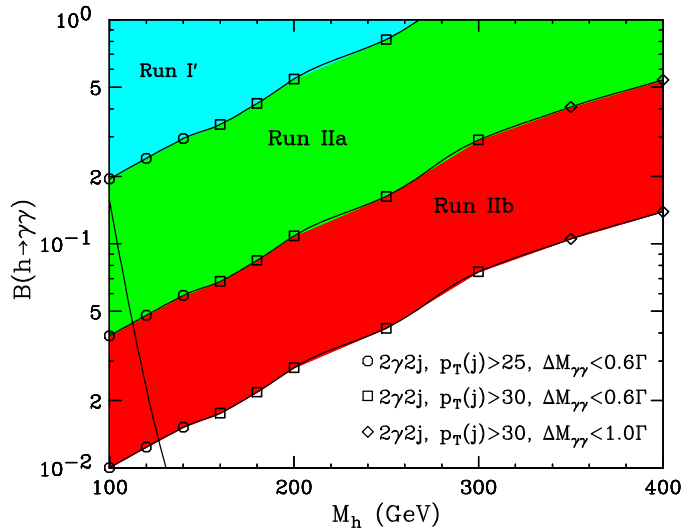


**FIGURE 6.** 95% CL upper limit on the branching ratio  $B(h \rightarrow \gamma\gamma)$ , with 0.1 (cyan), 2.0 (green) and  $30 \text{ fb}^{-1}$  (red), as a function of  $M_h$ . For each mass point, we compare the significance for both the inclusive and the exclusive channels with different cuts, and for the limit we choose the set of cuts which provides the best reach -  $\circ$ :  $2\gamma + 2j$ , with  $p_T(j) > 25 \text{ GeV}$  and  $w = 1.2\Gamma$ ;  $\square$ :  $2\gamma + 2j$ , with  $p_T(j) > 30 \text{ GeV}$  and  $w = 1.2\Gamma$ ; and  $\diamond$ :  $2\gamma + 2j$ , with  $p_T(j) > 30 \text{ GeV}$  and  $w = 2.0\Gamma$ . The solid line is the prediction for the branching ratio of a “bosonic” Higgs.

7. G. Abbiendi *et al.* [OPAL Collaboration], “Search for Higgs bosons and other massive states decaying into two photons in  $e^+e^-$  collisions at 189 GeV,” *Phys. Lett.* **B464**, 311 (1999), hep-ex/9907060; K. Ackerstaff *et al.* [OPAL Collaboration], “Search for Higgs bosons and new particles decaying into two photons at  $\sqrt{s} = 183 \text{ GeV}$ ,” *Phys. Lett.* **B437**, 218 (1998), hep-ex/9808014.
8. B. Lauer [DØ Collaboration] “A Search for High Mass Photon Pairs in  $p\bar{p} \rightarrow \gamma\gamma \text{ jet jet events at } \sqrt{s} = 1.8 \text{ TeV}$ ,” Ph.D. Thesis, University of Iowa, 1997 (unpublished).
9. B. Abbott *et al.* [D0 Collaboration], “Search for nonstandard Higgs bosons using high mass photon pairs in  $p\bar{p} \rightarrow \gamma\gamma + 2 \text{ jets at } \sqrt{s} = 1.8 \text{ TeV}$ ,” *Phys. Rev. Lett.* **82**, 2244 (1999), hep-ex/9811029.
10. P. J. Wilson [CDF collaboration], “Search for high mass photon pairs in  $p\bar{p}$  collisions at  $\sqrt{s} = 1.8 \text{ TeV}$ ,” FERMILAB-CONF-98-213-E *Contributed to 29th International Conference on High-Energy Physics (ICHEP 98), Vancouver, Canada, 23-29 Jul 1998*; J. A. Valls [CDF Collaboration], “Higgs Searches at the Tevatron in Run I,” preprint FERMILAB-CONF-99/263-E, *Proceedings of the International Europhysics Conference on High-Energy Physics (EPS-HEP99), Tampere, Finland, July 15-21, 1999*.
11. M. Spira, “Higgs boson production and decay at the Tevatron,” preprint DESY-98-159, hep-ph/9810289.
12. T. Sjöstrand, *Comp. Phys. Comm.* **82**, 74 (1994). We used version 6.136.
13. S. Abachi *et al.* [D0 Collaboration], “Studies of gauge boson pair production and trilinear couplings,” *Phys. Rev.* **D56**, 6742 (1997), hep-ex/9704004, and references therein.
14. B. Abbott *et al.* [D0 Collaboration], “A search for heavy pointlike Dirac monopoles,” *Phys. Rev. Lett.* **81**, 524 (1998), hep-ex/9803023.
15. J. Conway, talk given at the SUSY/Higgs Workshop meeting, Fermilab, May 14-16, 1998, additional information available at [www.physics.rutgers.edu/jconway/soft/shw/shw.html](http://www.physics.rutgers.edu/jconway/soft/shw/shw.html).
16. J. D. Lykken and K. T. Matchev, “Supersymmetry signatures with tau jets at the Tevatron,” *Phys. Rev.* **D61**, 015001 (2000), hep-ph/9903238; K. T. Matchev and D. M. Pierce, “Supersymmetry reach of the Tevatron via trilepton, like-sign dilepton and dilepton plus tau jet signatures,” *Phys. Rev.* **D60**, 075004 (1999), hep-ph/9904282.
17. A. Djouadi, J. Kalinowski and M. Spira, “HDECAY: A program for Higgs boson decays in the standard model and its supersymmetric extension,” *Comput. Phys. Commun.* **108**, 56 (1998), hep-ph/9704448.
18. M. Spira, “HIGLU: A Program for the Calculation of the Total Higgs Production Cross Section at Hadron Colliders via Gluon Fusion including QCD Corrections,” preprint DESY-T-95-05, hep-ph/9510347.

**TABLE 3.** The same as Table 1, but for a topcolor Higgs, i.e. gluon fusion events are included in the signal.

$M_h$ (GeV)	$\gamma\gamma + X$ bknd (fb)	Significance $S/\sqrt{B}$								
		$\gamma\gamma + X$	$\gamma\gamma + 1$ jet				$\gamma\gamma + 2$ jets			
			$p_T > 20$	$p_T > 25$	$p_T > 30$	$p_T > 35$	$p_T > 20$	$p_T > 25$	$p_T > 30$	$p_T > 35$
100.	271.7	54.3	43.4	44.6	45.1	42.5	33.6	37.8	36.4	32.1
120.	166.6	42.5	35.3	36.9	37.3	35.3	26.5	30.8	30.2	27.5
140.	103.0	35.5	30.4	32.1	33.0	31.6	22.3	25.6	25.1	22.0
160.	64.3	30.1	27.3	28.8	29.2	28.3	19.5	22.4	22.4	20.3
180.	40.5	24.5	22.4	23.8	24.5	23.8	15.7	18.2	18.3	17.6
200.	26.1	19.9	18.6	19.9	20.3	20.0	12.7	14.4	14.3	13.3
250.	9.4	12.9	12.5	13.3	13.6	13.4	8.4	9.7	10.2	9.8
300.	4.8	9.1	8.7	9.3	9.6	9.4	4.9	5.6	5.9	5.9
350.	2.3	8.4	7.9	8.4	8.4	7.9	4.0	4.1	4.5	4.5
400.	1.2	6.4	6.1	6.1	6.3	6.2	3.0	3.0	3.5	3.1

**TABLE 4.** The same as Table 3, but for a  $w = 2\Gamma$  mass window.

$M_h$ (GeV)	$\gamma\gamma + X$ bknd (fb)	Significance $S/\sqrt{B}$								
		$\gamma\gamma + X$	$\gamma\gamma + 1$ jet				$\gamma\gamma + 2$ jets			
			$p_T > 20$	$p_T > 25$	$p_T > 30$	$p_T > 35$	$p_T > 20$	$p_T > 25$	$p_T > 30$	$p_T > 35$
100.	453.4	47.7	37.6	38.9	39.5	36.9	29.0	33.0	31.6	27.1
120.	278.1	37.7	31.2	32.6	33.1	31.2	23.5	26.6	25.9	23.1
140.	171.9	31.4	26.7	28.2	29.0	27.9	19.2	22.1	22.0	19.4
160.	107.3	26.6	24.3	25.3	26.0	25.2	17.4	19.7	19.5	18.3
180.	67.6	22.3	20.5	21.7	22.1	21.6	14.2	16.2	16.8	15.4
200.	43.6	18.8	17.7	19.1	19.4	18.9	12.0	13.7	13.8	12.5
250.	15.7	12.8	12.1	13.2	13.4	13.1	8.2	9.3	10.0	9.6
300.	8.1	9.0	8.5	9.1	9.2	9.0	5.0	5.6	5.6	5.7
350.	3.9	8.3	7.6	8.1	8.1	7.9	4.0	4.7	4.6	4.4
400.	2.1	6.3	6.1	6.3	6.3	6.1	2.9	3.4	3.7	3.6

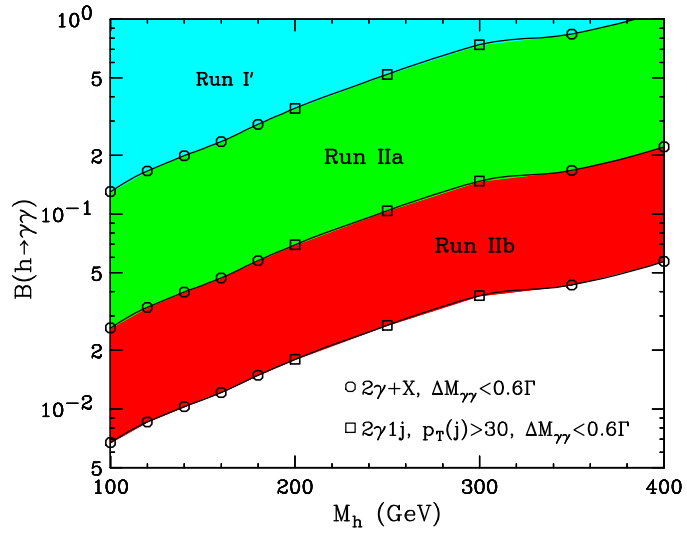


**FIGURE 7.** The same as Fig. 6, but for a topcolor Higgs, i.e. gluon fusion events are included in the signal. The channels with the best  $S/\sqrt{B}$  ratio are: o: inclusive  $2\gamma + X$ , and □:  $2\gamma + 1j$ , with  $p_T(j) > 30$  GeV; both with  $w = 1.2\Gamma$ .